HHS Public Access

Author manuscript

Oncogene. Author manuscript; available in PMC 2013 May 15.

Published in final edited form as:

Oncogene. 2012 November 15; 31(46): 4848–4858. doi:10.1038/onc.2011.644.

Inhibiting oncogenic signaling by sorafenib activates PUMA via GSK3β and NF-κB to suppress tumor cell growth

Crissy Dudgeon[1], **Rui Peng**[1], **Peng Wang**[1], **Andrea Sebastiani**[1], **Jian Yu**[2], and **Lin Zhang**[1]

[1]Department of Pharmacology and Chemical Biology, University of Pittsburgh Cancer Institute, University of Pittsburgh, Pittsburgh, PA

[2]Department of Pathology, University of Pittsburgh Cancer Institute, University of Pittsburgh, Pittsburgh, PA

Abstract

Aberrant Ras/Raf/MEK/ERK signaling is one of the most prevalent oncogenic alterations and confers survival advantage to tumor cells. Inhibition of this pathway can effectively suppress tumor cell growth. For example, sorafenib, a multi-kinase inhibitor targeting c-Raf and other oncogenic kinases, has been used clinically for treating advanced liver and kidney tumors, and also has shown efficacy against other malignancies. However, how inhibition of oncogenic signaling by sorafenib and other drugs suppresses tumor cell growth remains unclear. In this study, we found that sorafenib kills cancer cells by activating PUMA, a p53 target and a BH3-only Bcl-2 family protein. Sorafenib treatment induces PUMA in a variety of cancer cells irrespective of their p53 status. Surprisingly, the induction of PUMA by sorafenib is mediated by IκB-independent activation of NF-κB, which directly binds to the *PUMA* promoter to activate its transcription. NF-κB activation by sorafenib requires GSK3β activation, subsequent to ERK inhibition. Deficiency in PUMA abrogates sorafenib-induced apoptosis and caspase activation, and renders sorafenib resistance in colony formation and xenograft tumor assays. Furthermore, the chemosensitization effect of sorafenib is dependent on PUMA, and involves concurrent PUMA induction through different pathways. BH3 mimetics potentiate the anticancer effects of sorafenib, and restore sorafenib sensitivity in resistant cells. Together, these results demonstrate a key role of PUMA-dependent apoptosis in therapeutic inhibition of Ras/Raf/MEK/ERK signaling. They provide a rationale for manipulating the apoptotic machinery to improve sensitivity and overcome resistance to the therapies that target oncogenic kinase signaling.

Keywords

sorafenib; PUMA; apoptosis; NF-κB; GSK3β; colon cancer

Correspondence: Lin Zhang, the UPCI Research Pavilion, Room 2.42a, Hillman Cancer Center, 5117 Centre Ave., Pittsburgh, PA 15213. Phone: (412) 623-1009. Fax: (412) 623-7778. zhanglx@upmc.edu.

Introduction

Addictive oncogenic kinase signaling perpetuates tumor phenotypes, including sustained cell proliferation, insensitivity to apoptosis, and increased angiogenesis. The Ras/Raf/MEK/ERK pathway is aberrantly activated in most tumor cells due to *Ras* or *Raf* mutations (1). Sorafenib (Nexavar), an oral multi-kinase inhibitor that inhibits several aberrantly activated kinases in tumor cells, including c-Raf, B-Raf, PDGFR (platelet-derived growth factor receptor), and VEGFRs (vascular endothelial growth factor receptors) 1–3, has been used for the treatment of advanced kidney and liver tumors (2, 3). It has also been tested in hundreds of clinical trials against a variety of malignancies, including those of colon, lung, and breast. Unfortunately, the anticancer mechanisms of sorafenib and most targeted anticancer drugs remain poorly understood. Inevitable tumor recurrence due to acquired drug resistance has significantly limited clinical applications of targeted therapies.

Induction of apoptosis in cancer cells has emerged as a key effect of targeted therapies (4). For example, clinical response to EGFR (epidermal growth factor receptor) targeted therapy is correlated with induction of apoptosis in tumor cells, and defective apoptosis regulation contributes to resistance of EGFR targeted therapy (5). The anticancer effects of sorafenib are also thought to be mediated by apoptosis induction in cancer cells, in addition to its anti-proliferative and anti-angiogenic effects (6). Sorafenib kills a variety of tumor cells in vitro and in vivo, and its proapoptotic activity is significantly enhanced when combined with genotoxic drugs (7). Recent studies suggest that sorafenib-induced apoptosis is associated with downregulation of the antiapoptotic protein Mcl-1 and inhibition of eIF4E (eukaryotic translation initiation factor 4E) phosphorylation (8–10). However, Mcl-1 depletion alone is often insufficient to trigger apoptosis in solid tumor cells, and the timing of these changes does not correlate with that of apoptosis induction in sorafenib-treated cells (7). Therefore, how sorafenib triggers apoptosis in cancer cells remains unresolved.

PUMA (p53 upregulated modulator of apoptosis), a BH3-only Bcl-2 family member, functions as a critical initiator of apoptosis in cancer cells (11). Its transcription is directly activated by p53 in response to DNA damage. Lack of PUMA induction renders p53-deficient cancer cells refractory to conventional cytotoxic chemotherapeutic drugs (12). PUMA can also be induced in a p53-independent manner by a variety of non-genotoxic stimuli, such as the pan-kinase inhibitor UCN-01(13), the EGFR inhibitors gefitinib and erlotinib (14), and tumor necrosis factor-α (TNF-α) (15). p53-independent PUMA induction can be mediated by the transcription factors p73, FoxO3a (Forkhead Box O3a), and NF-κB (nuclear factor κB) (13–16). Upon its induction, PUMA potently induces apoptosis in cancer cells by antagonizing antiapoptotic Bcl-2 family members, such as Bcl-2 and Bcl-X_L, and activating the proapoptotic members Bax and Bak, which results in mitochondrial dysfunction and caspase activation cascade (17–19).

In this study, we found that sorafenib kills colon cancer cells in vitro and in vivo by activating PUMA through NF-κB. Our results shed light on the anticancer mechanism of sorafenib, and provide a rationale for manipulating PUMA and other apoptosis regulators to improve the efficacy of targeted therapies.

Results

Sorafenib selectively induces PUMA in cells expressing wildtype or mutant p53

We analyzed the effects of sorafenib in colorectal cancer cells because these cells were initially used for characterizing the anticancer activities of sorafenib (20, 21). Treating *p53*-wildtype (WT) HCT116 colon cancer cells with 5 to 20 μmol/L sorafenib strongly induced PUMA protein expression in a dose- and time-dependent manner (Figures 1a and b). *PUMA* mRNA was also induced by sorafenib (Figure 1c). The peak levels of *PUMA* mRNA and protein were detected at 16–24 hours following sorafenib treatment (Figures 1b and c). The induction of PUMA by sorafenib was found to be intact in *p53*-KO HCT116 cells (Figures 1a and c), and occurred in all of the colon cancer cells analyzed, including *p53*-WT Lim1405, Lovo, and RKO colon cancer cells, and *p53*-mutant DLD1 and HT29 colon cancer cells, as well as in HepG2 and Huh-7 hepatocellular carcinoma cells (Figure 1d). Furthermore, analysis of other Bcl-2 family members showed that sorafenib treatment did not induce the BH3-only proteins Bad, Bid, Bim, and Noxa, but led to degradation of Mcl-1 as previously reported (8), and a slight induction of Bcl-2 (Figure 1e). These results indicate that PUMA is selectively induced by sorafenib and may mediate its anticancer effects.

PUMA activation by sorafenib is mediated by NF-κB

We then investigated the mechanism by which sorafenib induces PUMA in the absence of p53. Knockdown of *c-Raf* by siRNA induced PUMA expression (Figures 2a and b), while depletion of other sorafenib targets, including *B-Raf*, *VEGFR2*, *PDGFR-β*, and *c-Kit*, did not increase PUMA expression (Supplementary Figure S1a and b), suggesting that PUMA induction by sorafenib results from c-Raf inhibition. FoxO3a, a transcription factor that can induce PUMA following its de-phosphorylation and nuclear translocation (22), remained phosphorylated in sorafenib-treated cells (Supplementary Figure S1c). Knockdown of FoxO3a by siRNA did not affect PUMA induction by sorafenib (Supplementary Figure S1d), indicating that FoxO3a is not involved in PUMA induction by sorafenib. The expression of p73, another transcription factor that can induce PUMA in p53-deficient cells (16), was unchanged after sorafenib treatment (data not shown). Sorafenib treatment also did not affect the expression and phosphorylation of the transcription factors STAT1 and STAT3 (Supplementary Figure S1e), which have been implicated in the effects of sorafenib (23).

The p65 subunit of NF-κB was recently identified as a transcriptional activator of PUMA in response to TNF-α treatment (15). Suppression of p65 expression by siRNA reduced PUMA levels following sorafenib treatment in both HCT116 and DLD1 cells (Figures 2c and d). In support of the requirement for p65, the induction of PUMA by sorafenib was also suppressed in *p65*-KO mouse embryonic fibroblasts (MEFs) (Figure 2d). Activation of NF-κB signaling is characterized by p65 phosphorylation on several residues and its subsequent translocation to the nucleus, where it activates transcription of target genes (24). We found that sorafenib treatment for 4–16 hours enhanced phosphorylation of S536, the major regulatory site of p65 (24), in both WT and *p53*-KO HCT116 cells (Figure 2e). Phosphorylation of S276, another site associated with p65 activation (24), was also increased after sorafenib treatment, while that of the controversial S468 site was unchanged

(Supplementary Figure S2a). Translocation of p65 to the nucleus was detected in cells treated with sorafenib or the control TNF-α by p65 immunofluorescence (Figure 2f), and by nuclear fractionation (Figure 3a). Consistent with NF-κB activation, transcription of *TNF-α*, a target of p65, was increased in response to sorafenib treatment (Figure 2g). But TNF-α secretion was not detected in sorafenib-treated cells (data not shown).

NF-κB binds to novel κB sites to directly activate *PUMA* transcription after sorafenib treatment

To determine how NF-κB activates *PUMA* transcription in response to sorafenib treatment, cells were pre-treated with BAY 11-7082, an NF-κB inhibitor suppressing p65 nuclear translocation (Figure 3a, *left*). NF-κB inhibition by BAY 11-7082 impeded PUMA induction by sorafenib or TNF-α (Figure 3a, *right*), suggesting that PUMA induction by sorafenib is mediated by p65 nuclear translocation. However, the change in p65 nuclear translocation detected by fractionation, which might be incomplete, seems to be less than that of PUMA induction. To determine whether NF-κB can directly activate *PUMA* transcription, *p53*-KO HCT116 cells were transfected with luciferase reporter constructs containing different regions of the *PUMA* promoter (Frags A-D; Figure 3b, *left*) (16). The previously identified NF-κB responsive element distal to Fragment D that is required for PUMA induction by TNF-α (15), was not activated in sorafenib-treated cells (data not shown). In contrast, the proximal 495-bp region of the *PUMA* promoter (Frags A and E) could be strongly activated upon sorafenib treatment (Figure 3b, *right*). Analysis of the DNA sequence in this region identified at least 5 previously unrecognized putative κB sites (Figure 3c). Mutations of all 5 κB sites completely blocked *PUMA* promoter activation by sorafenib treatment (Figure 3d), suggesting that multiple κB sites contribute to the activation of the *PUMA* promoter. Among the 5 sites analyzed, the third κB site (κB 3) seems to suppress the activity of *PUMA* promoter (Figure 3d). Chromatin immunoprecipitation (ChIP) revealed that p65 was recruited to the region containing the κB sites following sorafenib treatment (Figure 3e). Together, these results indicate that p65 directly binds to multiple κB sites in the proximal *PUMA* promoter region to drive its transcriptional activation in response to sorafenib treatment.

GSK3β-dependent, but IκB-independent p65 activation mediates PUMA induction by sorafenib

The canonical pathway of p65 activation is mediated by IκB phosphorylation and degradation, for example, in response to TNF-α treatment. Surprisingly, sorafenib treatment did not lead to IκB phosphorylation or degradation (Supplementary Figure S2b). Transfecting cells with IκBαM, a non-degradable mutant of IκB (15), did not affect sorafenib-induced PUMA expression (Figure 4a), suggesting that p65 activation and PUMA induction by sorafenib are not mediated by the canonical NF-κB pathway. Further analysis of other kinases known to activate NF-κB revealed that glycogen synthase kinase 3β (GSK3β) is involved in activating p65 following sorafenib treatment. Knockdown of GSK3β by siRNA suppressed sorafenib-induced p65 nuclear translocation determined by nuclear fractionation (Figure 4b), and by immunofluorescence (Supplementary Figure S3). GSK3β depletion also significantly reduced the levels of PUMA following sorafenib treatment in both HCT116 and RKO colon cancer cells (Figure 4c). Furthermore, sorafenib treatment

suppressed Ser9 phosphorylation of GSK3β, which inhibits its kinase activity (25), in both WT and *p53*-KO HCT116 cells (Figure 4d). It has been shown that the ERK kinase can prime GSK3β Ser9 phosphorylation to inhibit its activity (26). We found that sorafenib exposure strongly impaired phosphorylation of ERK1/2 (T202/Y204) throughout the course of treatment (Figure 4e). To determine whether ERK inhibition contributes to the activation of GSK3β, p65 and PUMA, we treated cells with the ERK inhibitor PD98059. ERK inhibition by PD98059 phenocopies sorafenib treatment in blocking GSK3β Ser9 phosphorylation, and promoting p65 phosphorylation and PUMA expression (Figure 4f). Together, these results demonstrate that PUMA induction by sorafenib is mediated by ERK inhibition, relief of GSK3β inhibition, and subsequent p65 activation.

PUMA is required for sorafenib-induced apoptosis

We then determined the role of PUMA induction in sorafenib-induced apoptosis. Apoptosis induced by 5–20 μmol/L sorafenib was markedly reduced in *PUMA*-KO cells but remained intact in *p53*-KO cells, in comparison with the parental HCT116 cells (Figure 5a and Supplementary Figure S4a). Annexin V/PI staining confirmed the suppression of sorafenib-induced apoptosis by the absence of PUMA (Figure 5b). Sorafenib-induced and PUMA-dependent apoptosis is not cell line-specific, and was also observed in DLD1 colon cancer cells (Figure 5c). In addition, sorafenib-induced apoptosis was found to be significantly reduced in *p65*-KO and *PUMA*-KO MEFs compared to WT MEFs (Figure 5c). PUMA deficiency inhibited sorafenib-induced mitochondrial events, including activation of caspases 3, 8, and 9 (Figure 5d), mitochondrial membrane permeabilization (Figure 5e), and cytochrome *c* release (Figure 5f). Reduced apoptosis in *PUMA*-KO cells does not seem to result from altered expression of other Bcl-2 family members or eIF4E (Supplementary Figure S4b). Furthermore, analysis of long-term cell survival by colony formation assay showed that *PUMA*-KO cells were less sensitive to sorafenib than WT cells (Figure 5g). Therefore, the killing effect of sorafenib on cancer cells is mediated by PUMA through the mitochondrial pathway.

PUMA mediates the chemosensitization effects of sorafenib

Sorafenib has mostly been used in combination with conventional cytotoxic therapies for cancer treatment. We reasoned that the chemosensitization effects of sorafenib are mediated by PUMA induction, because of the distinct mechanisms of PUMA activation by sorafenib and other drugs. Indeed, we found that sorafenib combined with cisplatin, which can enhance killing of various tumor cells (7), induced PUMA at a much higher level than sorafenib or cisplatin alone (Figure 6a). This is consistent with concurrent PUMA induction through both p53-dependent and -independent pathways by cisplatin and sorafenib, respectively. Accordingly, the level of apoptosis was also significantly higher in WT HCT116 cells, but not in *PUMA*-KO cells following the combination treatment (Figure 6b). A combination of sorafenib with UCN-01, a kinase inhibitor that induces PUMA through a pathway mediated by FoxO3a (13), also showed PUMA-dependent enhancement in apoptosis induction (Figure 6c). These results prompted us to test whether manipulating apoptosis by BH3 mimetics can sensitize cells to sorafenib. GX15-070, a BH3 mimetic compound analogous to PUMA in inhibiting all antiapoptotic Bcl-2 family members (27), markedly enhanced sorafenib-induced apoptosis in HCT116 cells (Figure 6d). GX15-070

also partially restored sorafenib sensitivity in *PUMA*-KO cells (Figure 6e). These data suggest that PUMA mediates the chemosensitization effects of sorafenib, and manipulating apoptosis can improve the therapeutic efficacy of sorafenib.

The in vivo therapeutic activity of sorafenib is PUMA-dependent

Sorafenib can effectively suppress the growth of colon cancer xenograft tumors (28). To determine if PUMA mediates the antitumor effects of sorafenib, WT and *PUMA*-KO HCT116 cells were injected subcutaneously into nude mice to establish xenograft tumors. Mice were then treated with 25 mg/kg sorafenib or the control vehicle by oral gavage for 7 consecutive days, as previously described (28). WT and *PUMA*-KO tumors were not different in growth after the control treatment (Figures 7a and b). Sorafenib treatment suppressed the growth of WT tumors by 60–80%, consistent with the previous report (28). In contrast, *PUMA*-KO tumors were significantly less sensitive to sorafenib treatment compared to WT tumors (Figures 7a, b, and Table S1), indicating that loss of PUMA suppressed the antitumor activity of sorafenib. Following sorafenib treatment, p65 phosphorylation and PUMA expression were found to be increased in xenograft tumors (Figure 7c). TUNEL staining revealed significant apoptosis induction in tumor tissues from the sorafenib-treated mice, but not the control mice. In contrast, apoptosis was barely detectable in the *PUMA*-KO tumors (Figure 7d). Analysis of apoptosis by active caspase 3 staining confirmed PUMA-dependent apoptosis in sorafenib-treated tumors (Figure 7e). Therefore, the in vivo antitumor activity of sorafenib is largely dependent on PUMA and involves NF-κB activation.

Discussion

Sorafenib is the first FDA-approved multi-kinase inhibitor drug that targets the Ras/Raf/MEK/ERK pathway, which is aberrantly activated in a majority of cancers due to *Ras* or *Raf* mutations (1). Sorafenib and other multi-kinase inhibitor drugs, such as sunitinib, can inhibit cell proliferation, promote apoptosis, and suppress tumor angiogenesis. While growth inhibition by sorafenib has been extensively characterized, the exact mechanism of sorafenib-induced apoptosis has not been clearly identified. Our results demonstrate that PUMA is activated following sorafenib exposure, and is necessary for sorafenib-induced apoptosis in colon cancer cells. Pharmacokinetic studies showed that sorafenib plasma concentrations could be as high as 10–20 μM (29). However, sorafenib is known to be bound to plasma proteins (7), and the biological active concentration of sorafenib in cultured cells may be higher than that in plasma of patients. backbone

Sorafenib-induced apoptosis was previously associated with degradation of Mcl-1 and inhibition of eIF4E phosphorylation (8–10). Mcl-1 depletion alone can induce apoptosis in hematopoietic cells (30), but is insufficient to induce apoptosis in the colon cancer cells we have studied, likely due to high levels of other antiapoptotic proteins such as Bcl-X_L. Induction of PUMA, on the other hand, can inhibit all antiapoptotic Bcl-2 family members, and activate the intrinsic apoptotic pathway (11). The increasing PUMA expression between 8–24 hours following sorafenib treatment also reconciles the previously noted “temporal disconnect” phenomenon (7), in which loss of eIF4E phosphorylation and Mcl-1 expression

occurs within the first 4 hours (10), much earlier than apoptotic events detected at 24 hours after sorafenib treatment. In addition to PUMA, other BH3-only proteins can also contribute to sorafenib-induced apoptosis. For example, sorafenib was shown to activate Bim to induce apoptosis in leukemia cells (31). The relative contributions of different BH3-only proteins are likely to be cell type-dependent.

PUMA-dependent apoptosis can be triggered by oncogene activation and functions as a safe-guide mechanism against oncogenic signaling (11). Induction of PUMA seems to be attributable to c-Raf inhibition by sorafenib. It is unexpected that the induction of PUMA relies on NF-κB, which is better known for its pro-survival activity. But NF-κB can clearly promote apoptosis under certain conditions (32). Recent studies have shown that the NF-κB signaling cascade can stimulate TNF-α secretion, which sets up a feedforward loop to promote apoptosis in response to extensive DNA damage (33). NF-κB activation by sorafenib does not involve IκB degradation, but is regulated by GSK3β through ERK inhibition. These results reinforce the multi-facet nature of NF-κB signaling, and suggest a potential role of NF-κB signaling in mediating responses to targeted therapies, which has not been appreciated.

Sorafenib is effective against a variety of malignancies such as renal cell carcinoma, hepatocellular carcinoma, breast cancer, colon cancer, non-small cell lung cancer, and melanoma (7). Currently, there are over 400 clinical trials involving sorafenib (http://www.clinicaltrials.gov). Our data demonstrate that PUMA-mediated apoptosis is critical for the anticancer activities of sorafenib in colon cancer cells, implying that PUMA induction can be used as a marker for therapeutic response to sorafenib, and possibly for other targeted drugs as well. Sorafenib has been most promising when used in combination with other chemotherapeutic agents. Depending on dosage and cell type, sorafenib combined with other drugs has additive and sometimes synergistic anticancer effects. In vitro and in vivo studies showed that sorafenib potentiates the effects of genotoxic agents, such as temozolomide, radiation, and melphalan (21, 34). Encouraging results have been obtained from clinical trials for combining sorafenib with genotoxic adjuvant treatments that involve cisplatin (35, 36). Our data suggest that the sensitization effect of sorafenib on cisplatin can be mediated by concurrent PUMA induction via both p53-dependent and -independent mechanisms. Sorafenib can also enhance tumor cell apoptosis in conjunction with non-genotoxic drugs, such as mTOR inhibitors (37), histone deacetylase inhibitors, and EGFR inhibitors (38). Ongoing clinical trials are testing combinations of sorafenib with erlotinib (39), and the farnesyltransferase inhibitor tipifarnib (40). It is perhaps understandable that these drugs work better in combination, because they likely induce PUMA through different pathways (14, 41, 42). Identifying effective drug combinations will be the key for clinical applications of sorafenib and other targeted drugs. PUMA induction may serve as a useful indicator for identifying such combination regimens.

Acquired drug resistance represents a major limitation of chemotherapy, and more so for targeted therapy. The pan-Bcl-2 inhibitor GX15-070 restored apoptosis in sorafenib-resistant *PUMA*-KO cells, suggesting that manipulating apoptotic pathways can help overcome sorafenib resistance. GX15-070 was also found to potentate the effect of sorafenib in chemo-resistant cancer cells lacking CD95 expression, or with overexpression of

antiapoptotic c-FLIP (43). The BH3 mimetic compound ABT-737 is effective in inducing apoptosis in HCC that would normally be cytostatic to sorafenib treatment (44). Another case of sorafenib resistance in HCC is shown to be caused by activation of PI3K/Akt signaling (45), and can be overcome by PI3K/Akt inhibition (46). We found that UCN-01, also a PI3K/Akt inhibitor, enhanced the killing effect of sorafenib in a PUMA-dependent manner, likely through FoxO3a-mediated PUMA induction (13). Together, these observations suggest that the PUMA-mediated apoptotic pathway might be explored to overcome resistance to targeted therapies. However, the clinical relevance of our findings remains to be established using more relevant cell models and human patient specimens.

In conclusion, we demonstrate that activation of PUMA by NF-κB mediates the apoptotic and anticancer effects of sorafenib in colon cancer cells in vitro and in vivo. PUMA induction may be a useful indicator for therapeutic response to sorafenib, and possibly other targeted drugs.

Materials and Methods

Cell culture and drug treatment

The human cancer cell lines, including HCT116, RKO, Lim2405, LOVO, HT29 and DLD1 colorectal cancer cells, and HepG2 and Huh-7 hepatocellular carcinoma cells, were obtained from American Type Culture Collection (Manassas, VA). Isogenic *p53*-knockout (KO) and *PUMA*-KO colon cancer cell lines were previously described (19, 47). All cell lines were cultured in McCoy's 5A modified media (Invitrogen) supplemented with 10% defined FBS (HyClone), 100 units/ml penicillin, and 100 μg/ml streptomycin (Invitrogen). Cells were maintained in a 37°C incubator at 5% CO_2. For drug treatment, cells were plated in 12-well plates at 20–30% density 24 hours prior to treatment. Sorafenib (LC Laboratories), BAY 11-7082, PD98059 (Merck Chemicals), GX15-070 (Cayman Chemical), UCN-01 (Sigma) were diluted with DMSO, cisplatin (Sigma) with 0.9% NaCl, and human TNF-α (R&D system) with PBS. For NF-κB inhibition, cells were pre-treated with BAY 11-7082 for 1 hour before sorafenib treatment.

Western blotting

Western blotting was performed as previously described (17). The antibodies used included those against PUMA (19), Akt, phospho-Akt (S473), Bad, Bid, active caspase 3, caspase 8, caspase 9, ERK, phospho-ERK (T202/Y204), IκB, phospho-IκB (S22/23), p65, phospho-p65 (Ser536, Ser276, and Ser468), phospho-FoxO3a, STAT1, phospho-STAT1 (Y701), STAT3, phospho-STAT3 (Y705), glycogen synthase kinase 3β (GSK3β), phospho-GSK3β (S9) (Cell Signaling), Bak, FoxO3a (Millipore), Bax, cytochrome oxidase subunit IV (Invitrogen), Mcl-1, IκB, cytochrome *c*, lamin A/C, eIF4E (Santa Cruz), β-actin (Sigma), Bim, Noxa, Bcl-2, α-tubulin (EMD Biosciences), Bcl-X_L (BD Transduction), and Bcl-w (Enzo Life Sciences). Western blot band intensities were quantified using ImageJ software (http://rsbweb.nih.gov/ij/).

Real-time reverse transcriptase (RT) PCR

Total RNA was isolated from sorafenib-treated cells using the Mini RNA Isolation II Kit (Zymo Research) according to the manufacturer's protocol. One μg of total RNA was used to generate cDNA using SuperScript II reverse transcriptase (Invitrogen). Real-time PCR was carried out as before for *PUMA* and *GAPDH* (13).

Transfection and siRNA knockdown

Cells were transfected with Lipofectamine 2000 (Invitrogen) according to the manufacturer's instructions. Knockdown experiments were performed 24 hours before sorafenib treatment using 400 pmoles of siRNA. *GSK3β* (sc-35527) and *VEGFR2* siRNA (sc-29318) were from Santa Cruz. All other siRNA, including those against human *p65* (15), *c-Raf* (AAGCACGCTTAGATTGGAATA-dTdT), *PDGFRβ* (GCAUCUUCAACAGCCUCUA-dTdT), *B-Raf* (ACAGAGACCUCAAGAGUAA-UU), *c-Kit* (GGCCGACAAAAGGAGAUCU-dTdT), and the control scrambled siRNA, were from Dharmacon. A non-degradable IκBα super repressor mutant (S32/36A; IκBαM) was previously described (15).

Luciferase assays

PUMA luciferase reporter constructs were generated by cloning genomic fragments (Fragments A-E) into the pBV-Luc plasmid as previously described (16). Mutations were introduced into the p65 binding sites of Fragment A using QuickChange XL site-directed mutagenesis kit (Agilent Technologies). For reporter assays, cells were transfected with the WT or mutant *PUMA* reporter along with the transfection control β-galactosidase reporter pCMVβ (Promega). Cell lysates were collected and luciferase activities were measured and normalized to those of pCMVβ as previously described (48). All reporter experiments were performed in triplicate and repeated thrice.

Chromatin immunoprecipitation (ChIP)

ChIP was performed using the Chromatin Immunoprecipitation Assay kit (Upstate Biotechnology) as previously described (47), with p65 antibody (Santa Cruz) for chromatin precipitation. The precipitates were analyzed by PCR using primers 5′-GTCGGTCTGTGTACGCATCG-3′ and 5′-CCCGCGTGACGCTACGGCCC-3′.

Analysis of NF-κB nuclear translocation

HCT116 cells pre-treated with BAY11-7082 or transfected with *GSK3β* siRNA were subjected to sorafenib or TNF-α treatment for 3 hours. NF-κB nuclear translocation was analyzed by nuclear fractionation and immunofluorescence. For nuclear fractionation, nuclear extracts were isolated from cells plated and treated in 75-cm^2 flasks using the NE-PER nuclear/cytoplasmic extraction kit (Thermo Fisher) according to the manufacturer's instructions, and probed by Western blotting for p65. For immunofluoscence, cells plated and treated in chamber slides were subject to primary staining with anti-p65 (Cell Signaling) overnight at 4°C, and secondary staining with the anti-rabbit AlexaFluor 488-conjugated secondary antibody (Invitrogen) for 1 hour at RT, as previously described (48). Images were acquired with an Olympus IX71 microscope.

Analysis of apoptosis

Nuclear staining with Hoechst 33258 (Invitrogen) was performed as previously described (49). Annexin V/propidium iodide (PI) staining was performed using annexin-Alexa 488 (Invitrogen) and PI as described (50). For analysis of cytochrome *c* release, mitochondrial and cytosolic fractions were isolated by differential centrifugation (18), followed by Western blotting for cytochrome *c*. For colony formation assays, the treated cells were plated in 12-well plates at appropriate dilutions, and allowed to grow for 10–14 days before staining with crystal violet (Sigma). For detection of mitochondrial membrane potential change, the treated cells were stained by MitoTracker Red CMXRos (Invitrogen) for 15 minutes at room temperature (RT), and then analyzed by flow cytometry.

Xenograft tumor experiments

All animal experiments were approved by the University of Pittsburgh Institutional Animal Care and Use Committee. Female 5–6 week-old Nu/Nu mice (Charles River) were housed in a sterile environment with micro isolator cages and allowed access to water and chow *ad libitum*. Mice were injected subcutaneously in both flanks with 4×10^6 WT or *PUMA*-KO HCT116 cells. Following tumor growth for 7 days, mice were treated daily with sorafenib at 25 mg/kg by oral gavage for 7 consecutive days. Sorafenib was dissolved in Cremephor EL/95% ethanol (50:50) as a 4× stock solution (20), and diluted to the final concentration with sterile water before use. Tumor growth was monitored by calipers, and tumor volumes were calculated according to the formula ½ × length × width^2. Mice were euthanized when tumors reached ~1.0 cm^3 in size. Tumors were dissected and fixed in 10% formalin and embedded in paraffin. TUNEL and active caspase 3 immunostaining was performed on 5 μM paraffin-embedded tumor sections as previously described (51), with an AlexaFluor 594-conjugated secondary antibody (Invitrogen) for signal detection.

Statistical Analysis

Statistical analyses were carried out using GraphPad Prism IV software. *P* values were calculated by the student's *t*-test and were considered significant if $P < 0.05$. The means ± one standard deviation (s.d.) were displayed in the figures.

Supplementary Material

Refer to Web version on PubMed Central for supplementary material.

Acknowledgments

We would like to thank Monica E. Buchanan, Brian Leibowitz, Mathew F. Brown and other lab members for critical reading and helpful discussion, Drs. Jennifer R. Grandis and Jing Hu for help with analyses of STAT1, STAT3, eIF4E, and GSK3β. This work is supported by NIH grants CA106348 and CA121105 and American Cancer Society grant RSG-07-156-01-CNE (L. Zhang); Flight Attendant Medical Research Institute, Alliance for Cancer Gene Therapy, and NIH grant CA129829 (J. Yu); NIH National Research Service Award postdoctoral fellowship grant F32CA139882 (C. Dudgeon); and China Scholarship Council (R. Peng). L. Zhang is a scholar of the V Foundation for Cancer Research.

Abbreviations

ChIP	chromatin immunoprecipitation
Cox IV	cytochrome oxidase subunit IV
EGFR	epidermal growth factor receptor
eIF4E	eukaryotic translation initiation factor 4E
HCC	hepatocellular carcinoma
FoxO3a	Forkhead Box O3a
KO	knockout
GSK3β	glycogen synthase kinase 3β
HDAC	histone deacetylase
MEFs	mouse embryo fibroblasts
NF-κB	nuclear factor κB
PDGFR	platelet-derived growth factor receptor
PUMA	p53 upregulated modulator of apoptosis
RT-PCR	reverse transcriptase-PCR
shRNA	small hairpin RNA
siRNA	small interfering RNA
TNF-α	tumor necrosis factor-α
VEGFR	vascular endothelial growth factor receptor
WT	wildtype

References

1. Vogelstein B, Kinzler KW. Cancer genes and the pathways they control. Nat Med. 2004; 10:789–799. [PubMed: 15286780]
2. Escudier B, Eisen T, Stadler WM, Szczylik C, Oudard S, Siebels M, et al. Sorafenib in advanced clear-cell renal-cell carcinoma. N Engl J Med. 2007; 356:125–134. [PubMed: 17215530]
3. Llovet JM, Ricci S, Mazzaferro V, Hilgard P, Gane E, Blanc JF, et al. Sorafenib in advanced hepatocellular carcinoma. N Engl J Med. 2008; 359:378–390. [PubMed: 18650514]
4. Green DR, Kroemer G. Pharmacological manipulation of cell death: clinical applications in sight? J Clin Invest. 2005; 115:2610–2617. [PubMed: 16200193]
5. Sordella R, Bell DW, Haber DA, Settleman J. Gefitinib-sensitizing EGFR mutations in lung cancer activate anti-apoptotic pathways. Science. 2004; 305:1163–1167. [PubMed: 15284455]
6. Wilhelm S, Carter C, Lynch M, Lowinger T, Dumas J, Smith RA, et al. Discovery and development of sorafenib: a multikinase inhibitor for treating cancer. Nat Rev Drug Discov. 2006; 5:835–844. [PubMed: 17016424]
7. Wilhelm SM, Adnane L, Newell P, Villanueva A, Llovet JM, Lynch M. Preclinical overview of sorafenib, a multikinase inhibitor that targets both Raf and VEGF and PDGF receptor tyrosine kinase signaling. Mol Cancer Ther. 2008; 7:3129–3140. [PubMed: 18852116]

8. Yu C, Bruzek LM, Meng XW, Gores GJ, Carter CA, Kaufmann SH, et al. The role of Mcl-1 downregulation in the proapoptotic activity of the multikinase inhibitor BAY 43–9006. Oncogene. 2005; 24:6861–6869. [PubMed: 16007148]
9. Rahmani M, Davis EM, Bauer C, Dent P, Grant S. Apoptosis induced by the kinase inhibitor BAY 43-9006 in human leukemia cells involves down-regulation of Mcl-1 through inhibition of translation. J Biol Chem. 2005; 280:35217–35227. [PubMed: 16109713]
10. Liu L, Cao Y, Chen C, Zhang X, McNabola A, Wilkie D, et al. Sorafenib blocks the RAF/MEK/ERK pathway, inhibits tumor angiogenesis, and induces tumor cell apoptosis in hepatocellular carcinoma model PLC/PRF/5. Cancer Res. 2006; 66:11851–11858. [PubMed: 17178882]
11. Yu J, Zhang L. PUMA, a potent killer with or without p53. Oncogene. 2008; 27 (Suppl 1):S71–83. [PubMed: 19641508]
12. Yu J, Yue W, Wu B, Zhang L. PUMA sensitizes lung cancer cells to chemotherapeutic agents and irradiation. Clin Cancer Res. 2006; 12:2928–2936. [PubMed: 16675590]
13. Dudgeon C, Wang P, Sun X, Peng R, Sun Q, Yu J, et al. PUMA induction by FoxO3a mediates the anticancer activities of the broad-range kinase inhibitor UCN-01. Mol Cancer Ther. 2010; 9:2893–2902. [PubMed: 20978166]
14. Sun Q, Ming L, Thomas SM, Wang Y, Chen ZG, Ferris RL, et al. PUMA mediates EGFR tyrosine kinase inhibitor-induced apoptosis in head and neck cancer cells. Oncogene. 2009; 18:2348–2357. [PubMed: 19421143]
15. Wang P, Qiu W, Dudgeon C, Liu H, Huang C, Zambetti GP, et al. PUMA is directly activated by NF-kappaB and contributes to TNF-alpha-induced apoptosis. Cell Death Differ. 2009; 16:1192–1202. [PubMed: 19444283]
16. Ming L, Sakaida T, Yue W, Jha A, Zhang L, Yu J. Sp1 and p73 Activate PUMA Following Serum Starvation. Carcinogenesis. 2008; 29:1878–1884. [PubMed: 18579560]
17. Ming L, Wang P, Bank A, Yu J, Zhang L. PUMA dissociates Bax and BCL-XL to induce apoptosis in colon cancer cells. J Biol Chem. 2006; 281:16034–16042. [PubMed: 16608847]
18. Yu J, Wang P, Ming L, Wood MA, Zhang L. SMAC/Diablo mediates the proapoptotic function of PUMA by regulating PUMA-induced mitochondrial events. Oncogene. 2007; 26:4189–4198. [PubMed: 17237824]
19. Yu J, Wang Z, Kinzler KW, Vogelstein B, Zhang L. PUMA mediates the apoptotic response to p53 in colorectal cancer cells. Proc Natl Acad Sci U S A. 2003; 100:1931–1936. [PubMed: 12574499]
20. Wilhelm SM, Carter C, Tang L, Wilkie D, McNabola A, Rong H, et al. BAY 43-9006 exhibits broad spectrum oral antitumor activity and targets the RAF/MEK/ERK pathway and receptor tyrosine kinases involved in tumor progression and angiogenesis. Cancer Res. 2004; 64:7099–7109. [PubMed: 15466206]
21. Plastaras JP, Kim SH, Liu YY, Dicker DT, Dorsey JF, McDonough J, et al. Cell cycle dependent and schedule-dependent antitumor effects of sorafenib combined with radiation. Cancer Res. 2007; 67:9443–9454. [PubMed: 17909054]
22. You H, Pellegrini M, Tsuchihara K, Yamamoto K, Hacker G, Erlacher M, et al. FOXO3a-dependent regulation of Puma in response to cytokine/growth factor withdrawal. J Exp Med. 2006; 203:1657–1663. [PubMed: 16801400]
23. Huang S, Sinicrope FA. Sorafenib inhibits STAT3 activation to enhance TRAIL-mediated apoptosis in human pancreatic cancer cells. Mol Cancer Ther. 2010; 9:742–750. [PubMed: 20197401]
24. Baud V, Karin M. Is NF-kappaB a good target for cancer therapy? Hopes and pitfalls. Nat Rev Drug Discov. 2009; 8:33–40. [PubMed: 19116625]
25. Cross DA, Alessi DR, Cohen P, Andjelkovich M, Hemmings BA. Inhibition of glycogen synthase kinase-3 by insulin mediated by protein kinase B. Nature. 1995; 378:785–789. [PubMed: 8524413]
26. Ding Q, Xia W, Liu JC, Yang JY, Lee DF, Xia J, et al. Erk associates with and primes GSK-3beta for its inactivation resulting in upregulation of beta-catenin. Mol Cell. 2005; 19:159–170. [PubMed: 16039586]

27. Zhang L, Ming L, Yu J. BH3 mimetics to improve cancer therapy; mechanisms and examples. Drug Resist Updat. 2007; 10:207–217. [PubMed: 17921043]
28. Wilhelm S, Chien DS. BAY 43-9006: preclinical data. Curr Pharm Des. 2002; 8:2255–2257. [PubMed: 12369853]
29. Clark JW, Eder JP, Ryan D, Lathia C, Lenz HJ. Safety and pharmacokinetics of the dual action Raf kinase and vascular endothelial growth factor receptor inhibitor, BAY 43-9006, in patients with advanced, refractory solid tumors. Clin Cancer Res. 2005; 11:5472–5480. [PubMed: 16061863]
30. Opferman JT, Iwasaki H, Ong CC, Suh H, Mizuno S, Akashi K, et al. Obligate role of anti-apoptotic MCL-1 in the survival of hematopoietic stem cells. Science. 2005; 307:1101–1104. [PubMed: 15718471]
31. Zhang W, Konopleva M, Ruvolo VR, McQueen T, Evans RL, Bornmann WG, et al. Sorafenib induces apoptosis of AML cells via Bim-mediated activation of the intrinsic apoptotic pathway. Leukemia. 2008; 22:808–818. [PubMed: 18200035]
32. Dutta J, Fan Y, Gupta N, Fan G, Gelinas C. Current insights into the regulation of programmed cell death by NF-kappaB. Oncogene. 2006; 25:6800–6816. [PubMed: 17072329]
33. Biton S, Ashkenazi A. NEMO and RIP1 control cell fate in response to extensive DNA damage via TNF-alpha feedforward signaling. Cell. 2011; 145:92–103. [PubMed: 21458669]
34. Augustine CK, Toshimitsu H, Jung SH, Zipfel PA, Yoo JS, Yoshimoto Y, et al. Sorafenib, a multikinase inhibitor, enhances the response of melanoma to regional chemotherapy. Mol Cancer Ther. 2010; 9:2090–2101. [PubMed: 20571072]
35. Sun W, Powell M, O'Dwyer PJ, Catalano P, Ansari RH, Benson AB 3rd. Phase II study of sorafenib in combination with docetaxel and cisplatin in the treatment of metastatic or advanced gastric and gastroesophageal junction adenocarcinoma: ECOG 5203. J Clin Oncol. 2010; 28:2947–2951. [PubMed: 20458043]
36. Kim C, Lee JL, Choi YH, Kang BW, Ryu MH, Chang HM, et al. Phase I dose-finding study of sorafenib in combination with capecitabine and cisplatin as a first-line treatment in patients with advanced gastric cancer. Invest New Drugs. 2010
37. Molhoek KR, Brautigan DL, Slingluff CL Jr. Synergistic inhibition of human melanoma proliferation by combination treatment with B-Raf inhibitor BAY43-9006 and mTOR inhibitor Rapamycin. J Transl Med. 2005; 3:39. [PubMed: 16255777]
38. Martinelli E, Troiani T, Morgillo F, Rodolico G, Vitagliano D, Morelli MP, et al. Synergistic antitumor activity of sorafenib in combination with epidermal growth factor receptor inhibitors in colorectal and lung cancer cells. Clin Cancer Res. 2010; 16:4990–5001. [PubMed: 20810384]
39. Lind JS, Dingemans AM, Groen HJ, Thunnissen FB, Bekers O, Heideman DA, et al. A multicenter phase II study of erlotinib and sorafenib in chemotherapy-naive patients with advanced non-small cell lung cancer. Clin Cancer Res. 2010; 16:3078–3087. [PubMed: 20395213]
40. Hong DS, Sebti SM, Newman RA, Blaskovich MA, Ye L, Gagel RF, et al. Phase I trial of a combination of the multikinase inhibitor sorafenib and the farnesyltransferase inhibitor tipifarnib in advanced malignancies. Clin Cancer Res. 2009; 15:7061–7068. [PubMed: 19903778]
41. Gomez-Benito M, Marzo I, Anel A, Naval J. Farnesyltransferase inhibitor BMS-214662 induces apoptosis in myeloma cells through PUMA up-regulation, Bax and Bak activation, and Mcl-1 elimination. Mol Pharmacol. 2005; 67:1991–1998. [PubMed: 15738311]
42. Zhang G, Park MA, Mitchell C, Hamed H, Rahmani M, Martin AP, et al. Vorinostat and sorafenib synergistically kill tumor cells via FLIP suppression and CD95 activation. Clin Cancer Res. 2008; 14:5385–5399. [PubMed: 18765530]
43. Martin AP, Park MA, Mitchell C, Walker T, Rahmani M, Thorburn A, et al. BCL-2 family inhibitors enhance histone deacetylase inhibitor and sorafenib lethality via autophagy and overcome blockade of the extrinsic pathway to facilitate killing. Mol Pharmacol. 2009; 76:327–341. [PubMed: 19483105]
44. Hikita H, Takehara T, Shimizu S, Kodama T, Shigekawa M, Iwase K, et al. The Bcl-xL inhibitor, ABT-737, efficiently induces apoptosis and suppresses growth of hepatoma cells in combination with sorafenib. Hepatology. 2010; 52:1310–1321. [PubMed: 20799354]

45. Chen KF, Chen HL, Tai WT, Feng WC, Hsu CH, Chen PJ, et al. Activation of PI3K/Akt signaling pathway mediates acquired resistance to sorafenib in hepatocellular carcinoma cells. J Pharmacol Exp Ther. 2011

46. Gedaly R, Angulo P, Hundley J, Daily MF, Chen C, Koch A, et al. PI-103 and sorafenib inhibit hepatocellular carcinoma cell proliferation by blocking Ras/Raf/MAPK and PI3K/AKT/mTOR pathways. Anticancer Res. 2010; 30:4951–4958. [PubMed: 21187475]

47. Wang P, Yu J, Zhang L. The nuclear function of p53 is required for PUMA-mediated apoptosis induced by DNA damage. Proc Natl Acad Sci U S A. 2007; 104:4054–4059. [PubMed: 17360476]

48. Yue W, Sun Q, Dacic S, Landreneau RJ, Siegfried JM, Yu J, et al. Downregulation of Dkk3 activates beta-catenin/TCF-4 signaling in lung cancer. Carcinogenesis. 2008; 29:84–92. [PubMed: 18048388]

49. Kohli M, Yu J, Seaman C, Bardelli A, Kinzler KW, Vogelstein B, et al. SMAC/Diablo-dependent apoptosis induced by nonsteroidal antiinflammatory drugs (NSAIDs) in colon cancer cells. Proc Natl Acad Sci U S A. 2004; 101:16897–16902. [PubMed: 15557007]

50. Li H, Wang P, Sun Q, Ding WX, Yin XM, Sobol RW, et al. Following Cytochrome c Release, Autophagy Is Inhibited during Chemotherapy-Induced Apoptosis by Caspase 8-Mediated Cleavage of Beclin 1. Cancer Res. 2011; 71:3625–3634. [PubMed: 21444671]

51. Qiu W, Wang X, Leibowitz B, Liu H, Barker N, Okada H, et al. Chemoprevention by nonsteroidal anti-inflammatory drugs eliminates oncogenic intestinal stem cells via SMAC-dependent apoptosis. Proc Natl Acad Sci U S A. 2010; 107:20027–20032. [PubMed: 21041628]

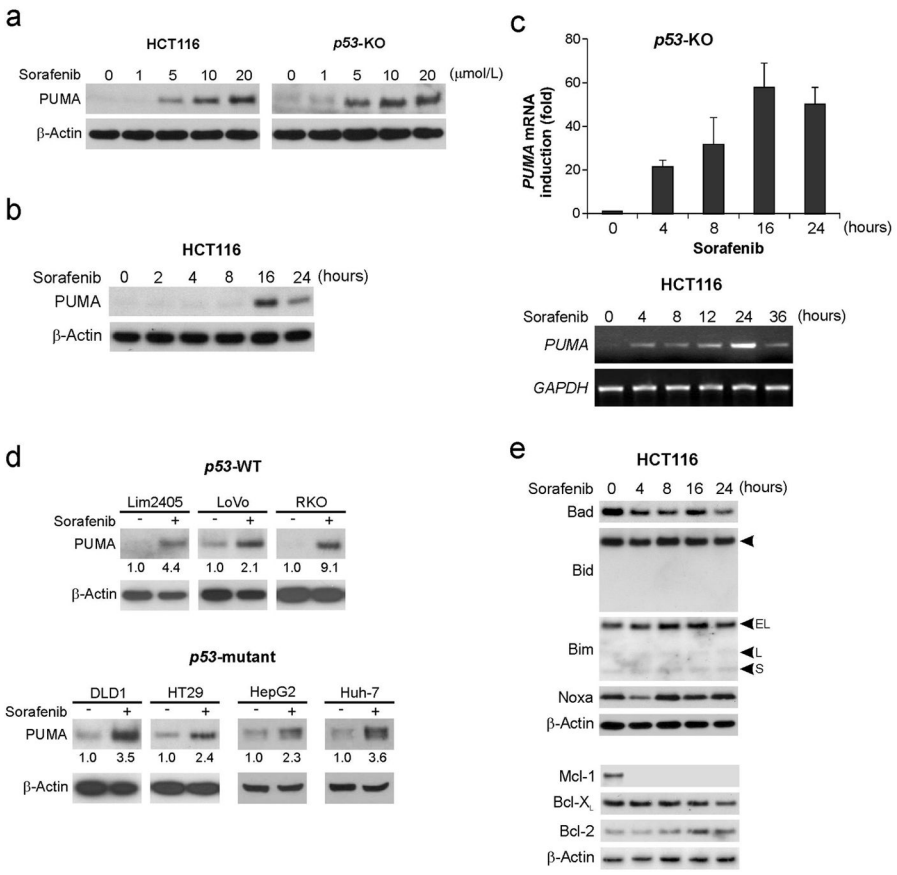

Figure 1. PUMA induction by sorafenib in cancer cells with or without p53

a. WT and *p53*-knockout (*p53*-KO) HCT116 colon cancer cells were treated with sorafenib at indicated concentrations for 24 hours. PUMA and β-actin expression was analyzed by Western blotting. **b.** Time course of PUMA protein induction in HCT116 cells treated with 20 μmol/L sorafenib was analyzed by Western blotting. **c.** *Upper*, time course of *PUMA* mRNA induction in *p53*-KO HCT116 cells treated with 20 μmol/L sorafenib was analyzed by real-time RT PCR; *Lower*, time course of *PUMA* mRNA induction in WT HCT116 cells treated with 20 μmol/L sorafenib was analyzed by RT PCR followed by gel electrophoresis, with *GAPDH* as a control. **d.** Indicated cancer cell lines with different *p53* status were treated with 20 μmol/L sorafenib for 24 hours. PUMA expression was analyzed by Western blotting. Except for HepG2 and Huh-7, which are hepatocellular carcinoma cells, all other cell lines are colorectal cancer cells. Relative PUMA expression of each sample, normalized to that of the loading control β-actin, is indicated, with that of the untreated cells arbitrarily set as 1.0. **e.** Western blot analysis of the expression of Bcl-2 family members at indicated time points in HCT116 cells treated with 20 μmol/L sorafenib.

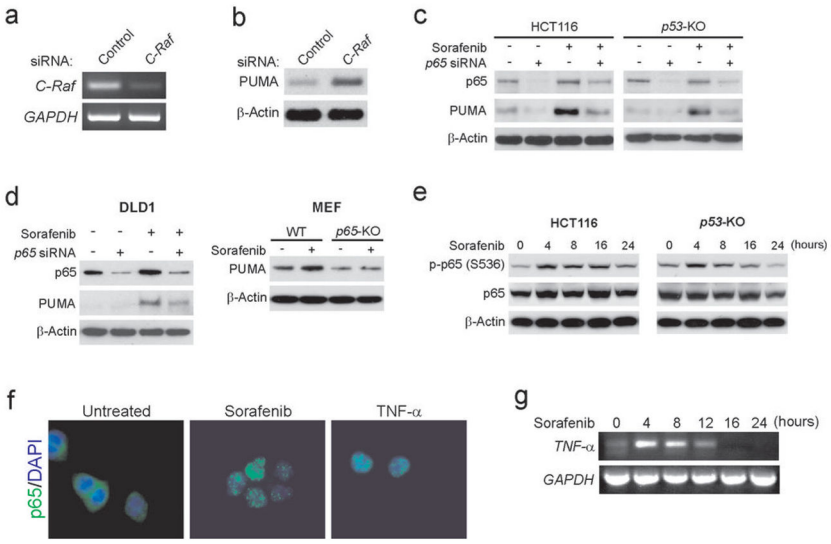

Figure 2. p65 is activated and required for *PUMA* induction following sorafenib treatment

a. HCT116 cells were transfected with a control scrambled siRNA or siRNA against *c-Raf*. Gene expression at 24 hours after siRNA transfection was analyzed by RT-PCR. **b.** Following siRNA transfection as in **a**, HCT116 cells were treated with 20 μmol/L sorafenib for 24 hours. PUMA expression was analyzed by Western blotting. **c.** WT and *p53*-KO HCT116 cells were transfected with either a control scrambled siRNA or a *p65* siRNA for 24 hours, and then treated with 20 μmol/L sorafenib for 24 hours. p65 and PUMA expression was probed by Western blotting. **d.** *Left*, DLD1 cells were transfected with control or *p65* siRNA, and then treated with 20 μmol/L sorafenib for 24 hours. p65 and PUMA expression was analyzed by Western blotting; *Right*, WT and *p65*-KO MEFs were treated with 1 μmol/L sorafenib for 24 hours. PUMA expression was analyzed by Western blotting. **e.** WT and *p53*-KO HCT116 cells were treated with 20 μmol/L sorafenib. Expression of p-p65 (S536), p65, and β-actin at indicated time points was analyzed by Western blotting. **f.** HCT116 cells were treated with 20 μmol/L sorafenib or 10 ng/mL TNF-α for 3 hours then fixed. Immunofluorescence was carried out as described in the Materials and Methods for p65 (green) and DAPI (blue). Representative pictures (400×) are shown. **g.** *TNF-α* expression in HCT116 cells treated with 20 μmol/L sorafenib was analyzed by RT-PCR, with *GAPDH* as a control.

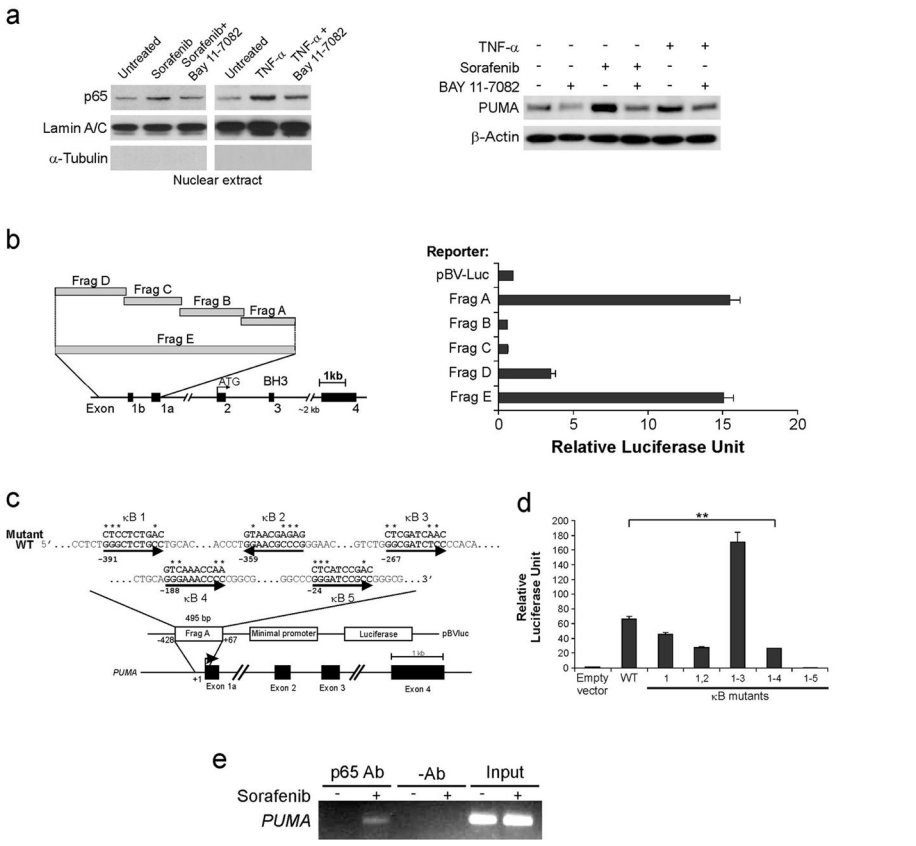

Figure 3. p65 directly binds to the *PUMA* promoter to activate its transcription following sorafenib treatment

a. HCT116 cells were treated with 10 μmol/L BAY11-7082 for 1 hour, and then with 20 μmol/L sorafenib or 10 ng/mL TNF-α. *Left*, nuclear fractions were isolated from cells treated with sorafenib or TNF-α for 3 hours, and analyzed for p65 expression by Western blotting. Lamin A/C and α-tubulin, which are expressed in nucleus and cytoplasm, respectively, were used as controls for loading and fractionation; *Right*, Western blot analysis of PUMA and β-actin expression in cells treated with sorafenib or TNF-α for 24 hours. **b.** *Left*, schematic representation of the genomic structure of *PUMA* highlighting the *PUMA* promoter Fragments A-E used in the luciferase experiment; *Right*, *p53*-KO HCT116 cells were transfected overnight with a luciferase reporter plasmid containing Fragments A-E of the *PUMA* promoter and then treated with 5 μmol/L sorafenib. Reporter activities were measured by luciferase assay 16 hours later. **c.** Schematic representation of the 5 p65 binding sites in Fragment A of the *PUMA* promoter. Asterisks represent the mutated nucleotides. **d.** *p53*-KO HCT116 cells were transfected overnight with a luciferase reporter plasmid containing indicated κB site mutants, and then treated and assayed as in **b. e.** Chromatin immunoprecipitation (ChIP) was performed using a p65-specific antibody on HCT116 cells following sorafenib (20 μmol/L) treatment for 8 hours. ChIP with no antibody (-Ab) was used to show specificity. PCR was carried out using primers surrounding the p65 binding sites in the *PUMA* promoter. Results in **b** and **d** were expressed as means ± SD of 3 independent experiments. ******, $P < 0.01$.

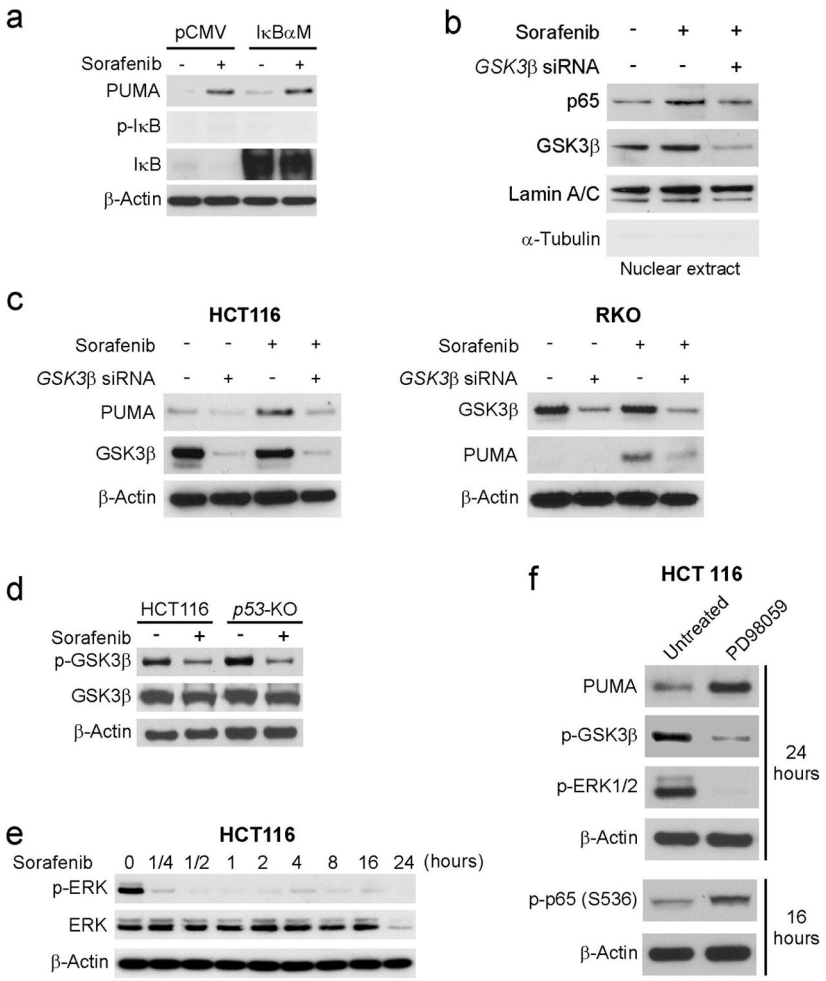

Figure 4. Sorafenib activates p65 to induce PUMA through GSK3β activation and ERK inhibition

a. HCT116 cells were transfected overnight with pCMV or IκBαM then treated with 20 μmol/L sorafenib for 24 hours. Expression of PUMA, p-IκB (S22/23), and IκB was analyzed by Western blotting. **b.** HCT116 cells were transfected with either a control scrambled siRNA or a *GSK3β* siRNA for 24 hours, and then treated with 20 μmol/L sorafenib for 3 hours. Nuclear fractions were isolated from cells treated with sorafenib and analyzed for p65 and GSK3β expression by Western blotting. **c.** Following transfection with the *GSK3β* siRNA as in **b**, HCT116 and RKO cells were treated with 20 μmol/L sorafenib for 24 hours. GSK3β and PUMA expression was analyzed by Western blotting. **d**. Western blot analysis of total GSK3β and p-GSK3β (S9) in WT and *p53*-KO HCT116 cells treated with 20 μmol/L sorafenib for 24 hours. **e**. Western blot analysis of p-ERK (T202/Y204) and ERK at indicated time points in HCT116 cells treated with 20 μmol/L sorafenib. **f.** HCT116 cells were treated with 25 μM of the ERK inhibitor PD98059 for 24 hours. Expression of PUMA, p-GSK3β (S9), p-ERK1/2 (T202/Y204) and p-p65 (S536) was analyzed by Western blotting.

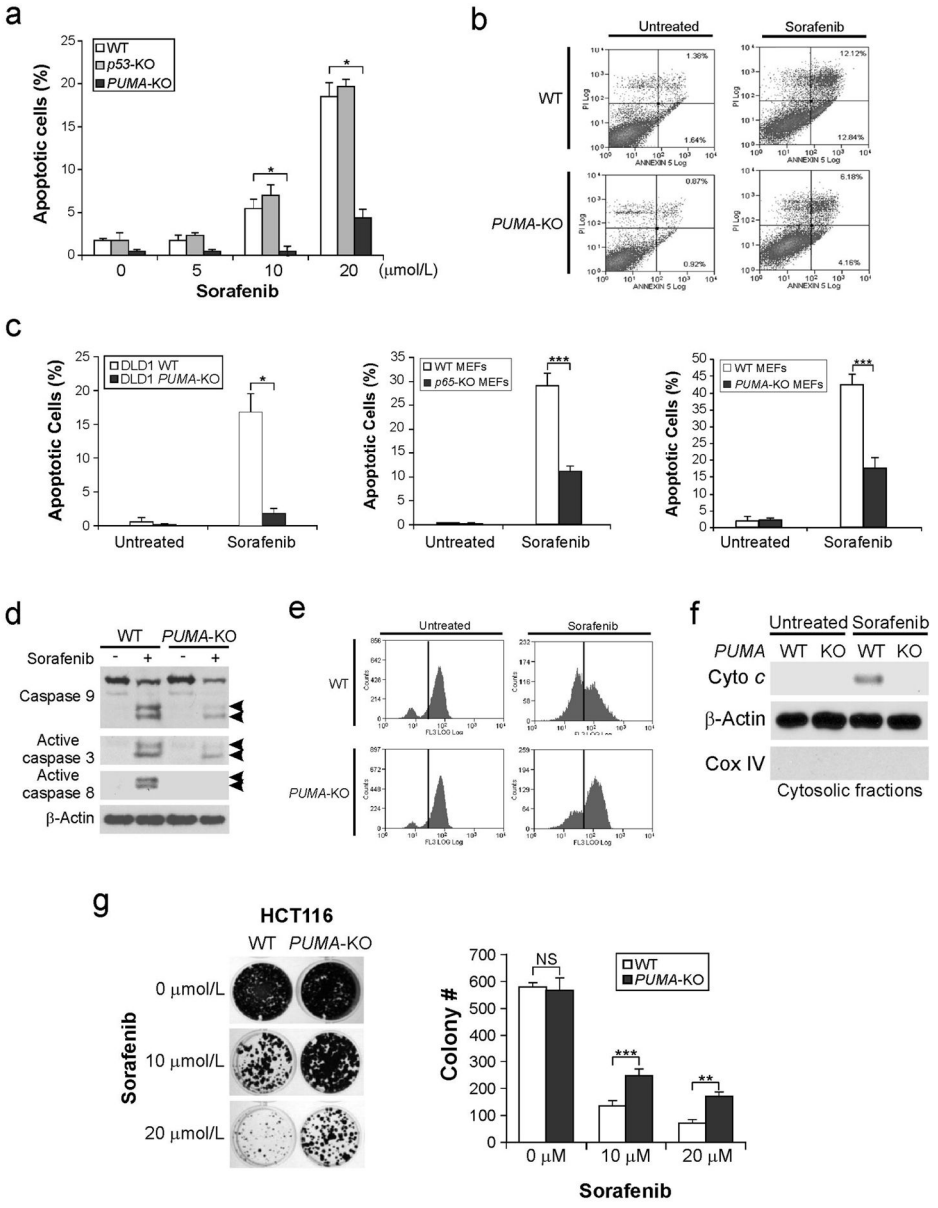

Figure 5. PUMA mediates the apoptotic and anticancer activities of sorafenib through the mitochondrial pathway

a. WT, *p53*-KO, and *PUMA*-KO HCT116 cells were treated with sorafenib at indicated concentrations for 48 hours. Apoptosis was analyzed by counting condensed and fragmented nuclei, following nuclear staining with Hoechst 33258. **b.** WT and *PUMA*-KO HCT116 cells were treated with 20 μmol/L sorafenib for 36 hours. Cells were stained with annexin V/PI and analyzed by flow cytometry. The percentages of annexin-positive cells are indicated in the two right quadrants. **c.** Comparison of apoptosis in WT and *PUMA*-KO DLD1 colon cancer cells (left), WT and *p65*-KO MEFs (middle), and WT and *PUMA*-KO MEFs following treatment with 20 μmol/L sorafenib for 48 hours. Apoptosis was analyzed by nuclear staining as in **a. d.** Western blot analysis of active caspase 3, caspase 8, and caspase 9 in WT and *PUMA*-KO HCT116 cells with or without sorafenib (20 μmol/L) treatment for

48 hours. Arrows indicate cleaved caspase fragments. **e.** After treatment of WT and *PUMA*-KO HCT116 cells with 20 μmol/L sorafenib for 36 hours, mitochondrial membrane potential was analyzed by staining with MitoTracker Red CMXRos, followed by flow cytometry. **f.** Cytosolic fractions isolated from WT and *PUMA*-KO HCT116 cells treated with 20 μmol/L sorafenib for 36 hours were probed for cytochrome *c* by Western blotting. α-Tubulin and cytochrome oxidase subunit IV (Cox IV), which are expressed in cytoplasm and mitochondria, respectively, were analyzed as the control for loading fractionation. **g.** Colony formation assay was done by seeding an equal number of WT and *PUMA*-KO HCT116 cells treated with 10 or 20 μmol/L sorafenib for 48 hours in 12-well plates, and then staining attached cells with crystal violet 14 days later. *Left*, representative pictures of colonies; *Right*, quantification of colony numbers. Results in **a, c** and **g** were expressed as means ± SD of 3 independent experiments. ***, $P < 0.001$; **, $P < 0.01$; *, $P < 0.05$; NS, not significant.

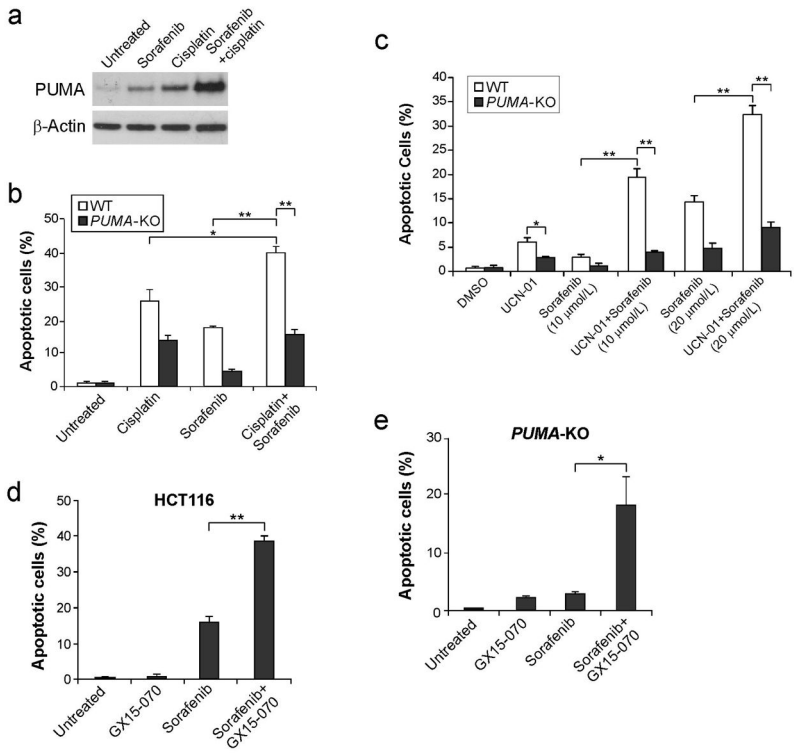

Figure 6. PUMA mediates the chemosensitization effects of sorafenib and enhances its anticancer activity

a. HCT116 cells were treated with 20 μmol/L sorafenib, 20 μmol/L cisplatin, or their combination for 24 hours. PUMA expression was analyzed by Western blotting. **b.** WT and *PUMA*-KO HCT116 cells were treated with 20 μmol/L sorafenib, 50 μmol/L cisplatin, or their combination for 48 hours. Apoptosis was determined by nuclear staining with Hoechst 33258. **c.** WT and *PUMA*-KO HCT116 cells were treated for 48 hours with 1 μmol/L UCN-01 with or without a combination with 10 or 20 μmol/L sorafenib. Apoptosis was analyzed by nuclear staining with Hoechst 33258. **d.** WT HCT116 cells were treated with 20 μmol/L sorafenib, alone or in combination with 5 μmol/L of the BH3 mimetic GX15-070. Apoptosis was determined by nuclear staining 48 hours after treatment. **e.** Apoptosis in *PUMA*-KO HCT116 cells treated with sorafenib alone or in combination with GX15-070 analyzed as in **d**. Results of nuclear staining in **b**-**e** were expressed as means ± SD of 3 independent experiments. ***, P <0.001; **, P <0.01; *, P <0.05.

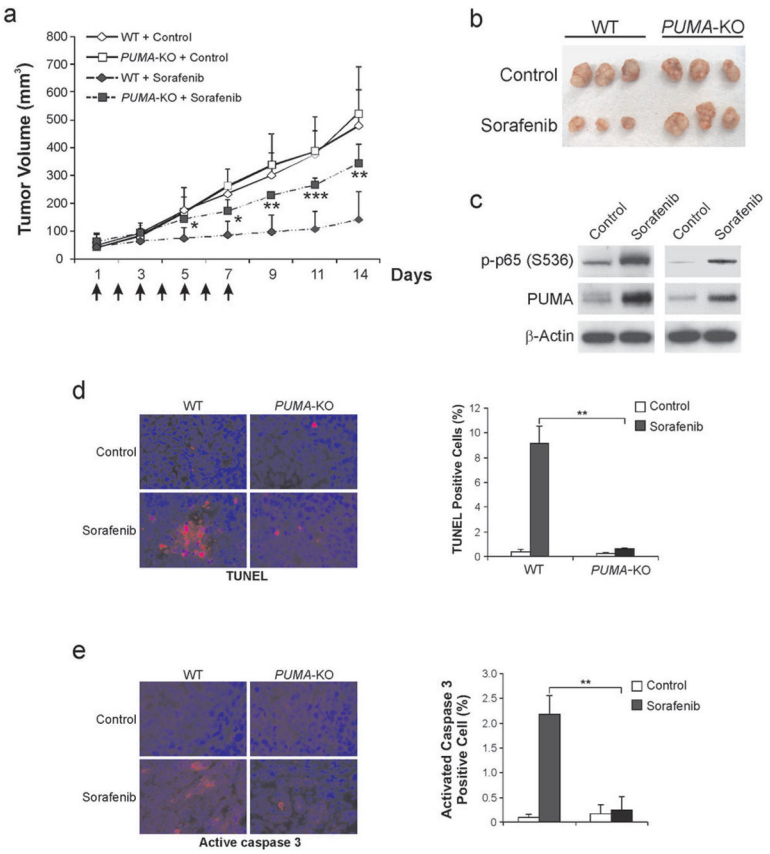

Figure 7. PUMA mediates the antitumor effect of sorafenib in a xenograft model

a. Nude mice were injected s.c. with 4×10^6 WT or *PUMA*-KO HCT116 cells. After 1 week, mice were oral gavaged with 25 mg/kg sorafenib or the control cremephor EL/ethanol buffer for 7 consecutive days. Tumor volume at indicated time points after treatment was calculated and plotted (n=5 in each group). Arrows indicate sorafenib injection. Statistical significance is indicated for comparison of sorafenib-treated WT and *PUMA*-KO tumors. *******, P <0.001; ******, P <0.01; *****, P <0.05. **b.** Representative tumors at the end of the experiment in **a. c.** WT and *PUMA*-KO HCT116 xenograft tumors were treated with 25 mg/kg sorafenib or the control buffer as in **a** for 4 consecutive days. p-p65 (S536) and PUMA expression in representative tumors was analyzed by Western blotting. **d.** WT or *PUMA*-KO HCT116 cells were treated with 25 mg/kg sorafenib or control buffer by oral gavage for 7 consecutive days as described in **a**. Paraffin-embedded tumor sections were analyzed by TUNEL staining. *Left*, representative TUNEL staining pictures (400×); *Right*, TUNEL-positive cells were counted and plotted. **e.** WT or *PUMA*-KO tumor tissues from mice treated as in **a** were analyzed by active caspase 3 staining. *Left*, representative staining pictures (400×); *Right*, active caspase 3-positive cells were counted and plotted. Results of **d** and **e** were expressed as means ± SD of 3 independent experiments. ******, P <0.01.